Wave Propagation in a Solid Ice Pack

ANTONY K. LIU AND ERIK MOLLO-CHRISTENSEN

Laboratory for Oceans, NASA/Goddard Space Flight Center, Greenbelt, Maryland

(Manuscript received 16 August 1987, in final form 1 June 1988)

ABSTRACT

The analysis presented in this paper was inspired by the report that the R/V *Polarstern* had encountered surface waves of large amplitude hundreds of kilometers inside the ice pack in the Weddell Sea. This paper presents analysis of processes that affect waves in an ice pack, namely the refraction of waves at the pack edge, the effects of pack compression on wave propagation, wave train stability and buckling stability in the ice pack. Sources of pack compresssion and interaction between wave momentum and pack compression are discussed. Viscous damping of propagating waves are also studied.

Significant results include the conditions for total reflection of waves at the pack edge, the strong effect of pack compressive stress on wave group speed, with the concomitant possibility of extreme local concentration of wave energy. The result that compressive stress in the pack leads to very rapid development of wave packets, through changes in the parameters for weakly nonlinear modulational instability of the wave field is also notable. The analysis suggests an explanation for the change in wave dispersion observed from the ship between the time of first arrival of the waves and after the pack was partially broken up by the first waves.

1. Introduction

It is well known that swell from the open sea penetrates into the ice pack and contributes to breakup of floes and to other processes that modify the ice cover, especially in the marginal ice zone. Squire (1984) has reported a combined theoretical, laboratory and field study of ice-coupled waves. Wadhams et al. (1986) have studied the change in the directional wave spectrum in the marginal ice zone, and they found an exponential decay in wave amplitude with distance from the pack edge.

The present work was inspired by a communication from E. Augstein, chief scientist on the R/V *Polarstern* for the 1986 winter cruise to the Weddell Sea. He reported that at a location in the ice pack 560 km from the ice edge, a series of waves of approximately one meter amplitude and 18 second period arrived, resulting in breakup of the ice pack. During the observed wave event there was evidence of active dynamics in the ice pack with ridging and rafting, resulting in ice thickness that locally was as much as 2 m with average thickness of 80 cm. The ship had difficulty moving with three engines working. When the waves first arrived, the wavelength was observed on radar, and as more waves arrived in the following hours, during the night, further observations of wavelength and period were made while the ship moved through the ice under the changed ice conditions.

The observations indicate that the first waves to arrive had a wavelength of approximately 250 m; this is much shorter than the wavelength of 18 second waves for open water conditions. Later, after the pack has been broken up by the waves, while the period remained the same, the wavelength had changed to a value near that to be expected from the open-water dispersion relation.

The change in wavelength for waves of nearly constant period suggests that the breakup of the ice field changed the dynamics of the wave field sufficiently to change the dispersion relationship. We suggest that as the ice was broken up by the first arrival of the waves the mean compressive stress in the ice pack decreased to near zero. The existence of compressive stresses in the ice pack has been long recognized in ship design for the Arctic. A well known example of a research vessel designed to withstand ice pack compression is the polar research ship *Fram* that was designed by Colin Archer for Fritjof Nansen in the nineteenth century. Pressure ridge formation is another well-known result of compressive stresses in the ice pack, the ridges are a result of ice floes being pushed up onto neighboring floes by compressive forces. The effects of mean compression on wave propagation in the ice pack were recognized by Mollo-Christensen (1983). He found that edge waves can have very low group velocity, and suggested it as an explanation of ice ride-up on shore.

We shall give the derivation of the dispersion relation for waves under pack compression, find the group velocity and calculate the critical mean compressive stress

Corresponding author address: Dr. Antony K. Liu, Laboratory for Oceans, NASA/Goddard Space Flight Center, Greenbelt, MD 20771.

for buckling failure in the pack. After applying the results of the analysis to the ice conditions observed in the Weddell Sea, we go on to examine the exchange of momentum between waves and the ice pack. Then we proceed to analyze the modulational stability of weakly nonlinear waves, and to discover that pack compression can change the rate of wave packet growth. For free surface gravity waves, the nonlinear tendency for variations in wave amplitude to grow was first discovered by Benjamin and Feir (1967). Their work initiated the growth of understanding of nonlinear wave processes that has occurred over the last two decades. We refer the reader to the paper by Yuen and Lake (1975), which gives some highlights of the work by Zakharov and Shabat (1972), and further to the book by Whitham (1975). Recently, surface waves of large amplitude beneath an elastic ice sheet has been studied by Forbes (1986), although he did not include the effects of compressive stress.

2. Dynamics of wave propagation

This analysis represents an extension of that of Wadhams (1973), with the effects of pack compression added (Mollo-Christensen 1983) and revised for the convenience of extending the analysis to momentum flux and nonlinear modulation processes. We shall neglect viscous effects, since the thickness of the boundary layer under the ice is much smaller than the wavelength, so there is little opportunity for viscosity to affect dispersion of the scale of a few wavelengths (Liu and Davis 1977). Later, we shall calculate wave attenuation caused by viscosity (see appendix A).

Take the water velocity field to be derived from a velocity potential $\phi(x, z, t)$ that satisfies the equation of continuity:

$$\nabla^2\phi(x, z, t) = 0. \tag{1}$$

A possible form of the solution is

$$\phi(x, z, t) = be^{kz}\cos(kx - \sigma t). \tag{2}$$

The vertical deflection of the ice–water interface is taken as

$$\eta(x, t) = a\sin(kx - \sigma t). \tag{3}$$

Considering the ice to be a thin ($kh \ll 1$) elastic plate of thickness h, the linearized relationship between the deflection and the water pressure immediately below the ice is (see Tse et al. 1978):

$$\left[\frac{Eh^3}{12(1-s^2)}\frac{\partial^4}{\partial x^4} + hP\frac{\partial^2}{\partial x^2} + \rho_I h\frac{\partial^2}{\partial t^2}\right]\eta(x, t) = P_a(x, t)_{z=\eta} = -\rho_w\left[\frac{\partial\phi}{\partial t} + g\eta\right]. \tag{4}$$

Bernoulli's equation has been used to express the pressure P_a in terms of velocity potential ϕ and deflection η, where g is the acceleration of gravity.

The notation used is the following:

- E Young's modulus of elasticity; for ice, $E = 6 \times 10^9$ N m^{-2};
- s Poisson's ratio; for ice, $s = 0.3$;
- P compressive stress in the ice pack; the stress for failure in pure compression is in the range of 10^6 N m^{-2} for sea ice (see Mellor 1983). In general, uniaxial compressive stress in ice is a function of ice type, strain rate and temperature under otherwise steady conditions. The maximum compressive stress for failure is three times the tensile stress for failure.

The density of sea ice is approximately $\rho_I = 0.9\rho_w$, where the density of sea water is approximately $\rho_w = 1025$ kg m^{-2}. The kinematic boundary condition at the underside of the ice is

$$\frac{\partial\eta}{\partial t} = \frac{\partial\phi}{\partial z} \tag{5}$$

to a linear approximation on the plane $z = 0$. Substituting from Eqs. (2), (3) and (5) into (4) yields the dispersion relation

$$\sigma^2(k) = \left[gk + \frac{Eh^3k^5}{12(1-s^2)\rho_w} - \frac{Phk^3}{\rho_w}\right]\Big/\left(1 + \frac{\rho_I hk}{\rho_w}\right) = (gk + Bk^5 - Qk^3)/(1 + kM). \tag{6}$$

The B, Q and M denote the effects that modify the frequency due to bending, compression, and the inertia of the ice respectively. They are defined by

$$B = \frac{Eh^3}{12(1-s^2)\rho_w}, \quad Q = \frac{Ph}{\rho_w}, \quad M = \frac{\rho_I h}{\rho_w}.$$

For zero compressive stress, Eq. (6) reduces to the dispersion relation found by Wadhams (1973).

3. Buckling

The breakup of the ice cover, as observed from the *Polarstern*, resulted from the additional stresses imposed by the waves causing structural failure. Failure can be a result of the action of combined stresses due to waves and structural instability, as exemplified by buckling in the presence of waves. Buckling is a lateral divergence of an elastic plate that initially grows exponentially with time and which, when the deflection has grown sufficiently large, results in structural failure. For an ice pack under a mean compressive stress below the failure stress level, additional stresses caused by bending due to waves may bring the local stress to the failure level. We suggest that this is what happened in the observed wave event.

Before one can suggest that the compressive stress in the pack was sufficient to give a very small value of

group velocity, one has to verify the buckling of the pack would not occur at a lower stress. The analysis proceeds as follows. From Eq. (6), it is apparent that the frequency can become imaginary for sufficiently high compressive stress. This will then lead to deflections that increase exponentially with time. The critical compressive stress for the instability known as buckling is

$$P_B = \frac{\rho_w}{h}\left[\frac{Eh^3k^4}{12(1-s^2)\rho_w} + g\right]\Big/k^2. \quad (7)$$

Note that this critical compressive stress is higher than the classical Euler buckling load for a beam that is not supported laterally by buoyancy. The critical Euler buckling stress for an unsupported beam is found from Eq. (7) by setting the acceleration of gravity to zero, and this gives

$$P_E = Eh^2k^2/[12(1-s^2)]. \quad (8)$$

It is evident that buckling depends upon wavenumber, and the minimum value of P_B for a floating ice sheet is found from Eq. (7) to be

$$P^2_{B_{\min}} = Eh\rho_w g/[3(1-s^2)]. \quad (9)$$

The corresponding wavenumber is

$$k_B{}^4 = 12\rho_w g(1-s^2)/(Eh^3). \quad (10)$$

This establishes the minimum compressive stress needed for the buckling of an infinitely long floating beam and also the wavelength at which buckling occurs. We are therefore ready to determine the critical stress at which the energy flux becomes zero, that is the compressive stress that gives zero group velocity.

4. Group velocity

Since wave energy propagates at group velocity, group velocity plays a fundamental role in wave propagation. When the group velocity decreases with distance, there will be accumulation of wave energy due to flux convergence, this can cause high wave amplitude locally. We suggest that this has been a contributory cause to the high wave amplitudes observed from the *Polarstern*.

From Eq. (6), the value of group velocity C_g is found to be

$$C_g = \frac{\partial\sigma}{\partial k} = [g + (5 + 4kM)Bk^4 - (3 + 2kM)Qk^2]/[2\sigma(1 + kM)^2]. \quad (11)$$

Note that the group velocity can take on the value of zero for a compressive stress P in excess of a critical value P_{crit}, given by

$$P_{\text{crit}} = \rho_w Q_c/h = \rho_w[g + (5 + 4kM)Bk^4]/[h(3 + 2kM)k^2]. \quad (12)$$

When $P_{\text{crit}} < P_B$ waves with a propagation phase can still exist but their group velocity can vary and, for $P = P_{\text{crit}}$, become vanishingly small. When the group velocity varies in the wave propagation direction from a positive value to a small value, there will be accumulation of wave energy. An infinite wave train of initially constant amplitude, entering from a distance, would attain singular amplitude where it encountered a place of zero group velocity. This is a possible mechanism that may explain the local occurrence of large amplitude waves in the ice pack. While linear theory looses its validity at large wave amplitude, the fact that zero group velocity can occur at lower compressive stress in the pack than the critical stress for buckling instability does suggest that very low group velocity may have caused focusing and have contributed to the observed Weddell Sea wave event.

5. Application of the analysis to the events observed in the Weddell Sea

The results of the preceding analysis will now be applied to the wave observations from the *Polarstern*. The observed wave period was 18 s, and the wavelength observed at the initial arrival of the waves was approximately 250 m, while the ice thickness was 2 m in the ridging and rafting area.

In the absence of ice, the wavelength for this wave period would be approximately 510 m; we suggest that the smaller observed wavelength must be due to the combined effects of pack flexural stiffness and pack compression. The only unknown term in the dispersion relation [Eq. (6)] is the compression term. Solving for this and listing all the terms, the following values are obtained for reference.

$$\text{Flexure:} \quad Bk^5 = Eh^3k^5/[12(1-s^2)\rho_w] = 4.2 \times 10^{-2}\ \text{s}^{-2}$$

$$\text{Compression:} \quad Qk^3 = Phk^3/\rho_w = 3.1P \times 10^{-8}\ \text{s}^{-2}$$

$$\text{Gravity:} \quad gk = 2.45 \times 10^{-1}\ \text{s}^{-2}$$

$$\text{Inertia:} \quad M = \rho_I h/\rho_w = 1.8\ \text{m}$$

The corresponding value of the compressive stress is $P = 5.1 \times 10^6\ \text{N m}^{-2}$. This value is less than the stress for compressive failure, and also less than the buckling stress. The buckling stress can be obtained from Eq. (9) as $P_{B_{\min}} = 6.7 \times 10^6\ \text{N m}^{-2}$, which occurs for a wavelength of 900 m approximately.

From the list of the magnitudes of the terms, it is to be noted that the compression effect is the main cause of departure from the free surface dispersion relation, where only gravity and inertia enter. Substituting the parameters into the expression for group velocity [Eq. (11)] results in $C_g \approx 0\ \text{m s}^{-1}$. The group velocity being nearly zero, one can conclude that wave energy accumulation must have occurred in the area of high compressive stress. The stress calculated with the observed

wave period and wavelength from the dispersion relation, with the resulting calculated zero value of group velocity, helps explain the large wave amplitudes that were observed. When the ice thickness decreases to one meter, the group velocity calculated from Eq. (11) increases to 2.4 m s^{-1}.

Observations of wavelength from a ship are not always precise, especially when an unexpected, short duration event occurs. It is therefore important to examine the sensitivity of the dispersion to variations in wavelength. We take the observed wave period to be correct, since this observation can be made by a person anywhere on board who feels the motion of the ship and has access to a watch.

Figure 1a shows the variation in compressive stress with wavelength λ calculated from Eq. (6) for waves of period $T = 18$ s. Note that the rate of change in compressive stress with wavelength is a maximum near zero compressive stress and is smaller for higher stress. The group velocity (solid line) and the phase speed (dotted line) for 18 s period waves are plotted as functions of wavelength in Fig. 1b. For reference, Fig. 1b also shows the group velocity for a constant compressive stress of $P = 5.1 \times 10^6$ N m^{-2} (dashed line).

Because the calculated compressive stress in the pack was near both the critical stress for buckling and the stress for compressive failure, the observed breakup of the ice pack and the rafting may be attributed to a combination of failure modes. Our analysis is linear and is only valid for infinitesimal wave amplitudes. Finite amplitude waves may be able to induce buckling below the critical stress for linear buckling instability.

The rafting process can be driven by the compressive stress that causes acceleration of some of the ice floes, and the rafting activity may persist for a short time after the compressive stress is relieved. Therefore, this process will result in the formation of open leads. Not all the rafting need to be caused by the mean compressive stress in the ice pack. The waves also contain momentum. When wave energy is destroyed by a combination of compressive failure, ice breaking and the dissipation that would be associated with pack failure, the wave momentum would have to be transferred partly to the water velocity field, and the rest to pack compression or local acceleration of ice floes. This, in turn, may contribute to rafting.

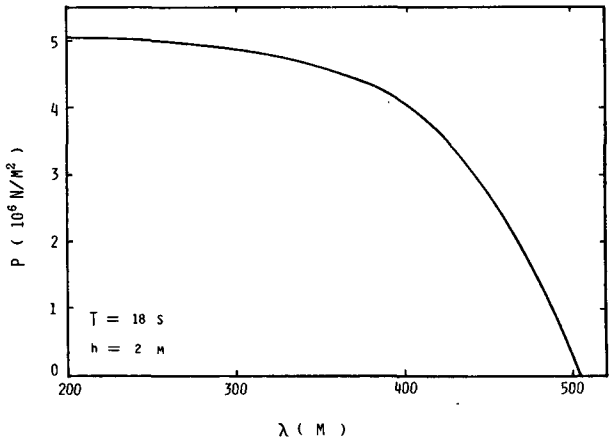

FIG. 1a. Ice compressive stress effects on wavelength λ calculated from Eq. (6) with ice thickness $h = 2$ m and wave period $T = 18$ sec.

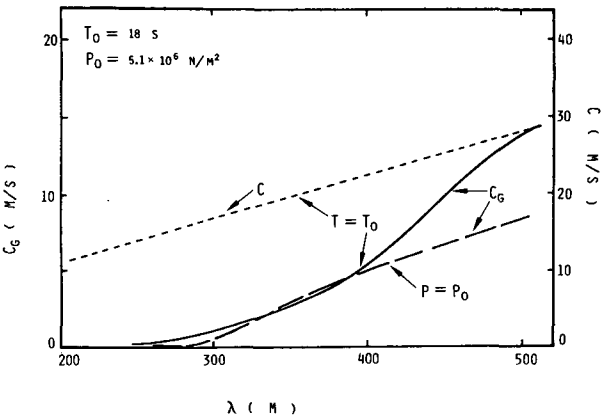

FIG. 1b. Group velocity (solid line) and phase speed (dotted line) as a function of wavelength with $T_0 = 18$ sec. Group velocity (dashed line) as a function of wavelength for a fixed compressive stress $P_0 = 5.1 \times 10^6$ N m^{-2}.

An area of rafting would change the wave group velocity, possibly giving rise to caustic formation for waves in a certain frequency range. If circumstances should form a lens-shaped area of increased ice thickness, spatial focusing could occur, the focal distance being dependent upon wave frequency. Pack modification by breakup and rafting is likely to occur in a focal region. The interaction between wave momentum and the mean state of the ice pack and flow field will be discussed next.

6. Momentum transfer by wave–ice interaction

Waves carry momentum, and when wave amplitude changes, the wave momentum has to show up as forces on the fluid and ice and/or as mean momentum in the pack and the water. It is therefore of interest to consider the exchange of momentum between waves and ice pack stresses for slowly varying wave and ice parameters.

From the boundary condition at the bottom of the ice, Eq. (4) can be written

$$\left(B\frac{\partial^4}{\partial x^4} + Q\frac{\partial^2}{\partial x^2} + M\frac{\partial^2}{\partial t^2} + g\right)\eta = -\frac{\partial \phi}{\partial t}. \quad (13)$$

For an ice deflection wave of the form given by Eq. (3), the velocity potential is

$$\phi = -a[(Bk^4 - Qk^2 - M\sigma^2 + g)/\sigma] \times e^{kz}\cos(kx - \sigma t). \quad (14)$$

The corresponding horizontal velocity just under the ice is

$$u = \frac{\partial \phi}{\partial x} = a[Bk^4 - Qk^2 - M\sigma^2 + g)/C] \times e^{kz} \sin(kx - \sigma t). \quad (15)$$

The wave momentum N is then given by (Phillips 1977)

$$N = -\rho_w \overline{\phi \frac{\partial \eta}{\partial x}} = \frac{1}{2} a^2 \rho_w (Bk^4 - Qk^2 - M\sigma^2 + g)/C \quad (16)$$

where $C = \sigma/k$, and the overbar denotes a time average on the plane $z = 0$ of the linearized solution.

Let us consider very slow variations of ice conditions with distance. That is, the length scale of variations of ice conditions and wave parameters is much longer than the wavelength. Then the rate of change of momentum with distance x can be expressed by

$$\begin{aligned} N' &= \frac{\partial N}{\partial x} \\ &= \frac{\rho_w}{2} \frac{\partial (a^2)}{\partial x} (Bk^4 - Qk^2 - M\sigma^2 + g)/C \\ &\quad + \frac{\rho_w}{2} a^2 \left(\frac{\partial B}{\partial x} k^4 - \frac{\partial Q}{\partial x} k^2 - \frac{\partial M}{\partial x} \sigma^2 \right) \Big/ C \\ &\quad + \frac{\rho_w}{2} a^2 (5Bk^4 - 3Qk^2 - M\sigma^2 + g) \frac{\partial k}{\partial x} \Big/ \sigma. \end{aligned} \quad (17)$$

For $kM \ll 1$, it can be shown from Eq. (11)

$$g + 5Bk^4 - 3Qk^2 = 2C_g \sigma. \quad (18)$$

Neglecting the terms

$$k^2 \frac{\partial B}{\partial x} \ll \frac{\partial Q}{\partial x}, \quad C^2 \frac{\partial M}{\partial x} \ll \frac{\partial Q}{\partial x},$$

as being small, the dominant terms in the spatial derivative of wave momentum are

$$N' = \frac{\rho_w}{2} [(a^2)'(Bk^4 - Qk^2 - M\sigma^2 + g)/C - a^2 Q' k^2/C + 2a^2 C_g k'] \quad (19)$$

where the primes indicate x-derivatives for slow variations.

The condition for conservation of momentum, i.e., $N' = 0$ is then

$$(a^2)'(Bk^4 - Qk^2 - M\sigma^2 + g) = a^2 k^2 Q' - 2a^2 C C_g k'. \quad (20)$$

This shows the relationship between the slow spatial rate of change of wave amplitude and the space derivative of compressive stress in the pack. Therefore, when the group velocity is very small at high compressive stress area, the wave energy density will increase with distance under conditions where the compressive stress in the pack is increasing in the wave propagation direction. We have neglected the effects of dissipation on wave amplitude. But dissipation can only redistribute momentum and cannot destroy it. More frequent ridge formation observed after the ice breakup may be caused by the transfer of wave momentum to the ice pack compression.

7. Nonlinear effects on wave development

The preceding analysis of wave propagation only considered linear effects and neglected the nonlinear terms in the equations. This gives good approximations for wave propagation over moderate distances, such as a few tens of wavelengths. For propagation over longer distances, the nonlinear effects will accumulate and give rise to wave packet formation and possibly consequent wave breaking. For waves in an ice pack, the ice may break at large wave amplitude.

Here we shall discuss the consequences of varying amplitude and finite amplitude for waves on an ice covered ocean. First, the envelope function $S(x, t)$ for the wave field, with the relationship to surface deflection $\eta(x, t)$, is defined by

$$\eta(x, t) = \mathrm{Re}[S(x, t) \exp i(kx - \sigma t)]. \quad (21)$$

The complex envelope function S can be shown to satisfy the nonlinear, cubic Schrödinger equation (Mei 1983)

$$\frac{\partial S}{\partial t} + i\beta \frac{\partial^2 S}{\partial x^2} + i\gamma S^2 S^* = 0. \quad (22)$$

The asterisk indicates the complex conjugate. We shall next examine how the coefficients in the equation change for an ice-covered ocean.

In general, the effect of pack compression can, under some circumstances, limit the distance required for the nonlinear effects to develop and thus further limit the range of validity of results of linear analysis. It is especially noteworthy we find that unstable wave packets can under favorable condition grow over a hundred times faster in the ice pack than in open water.

In this analysis, we will continue to neglect viscosity, so that we can assume irrotationality and continue to represent the water velocity field in terms of a velocity potential $\phi(x, z, t)$, with velocity components

$$u = \frac{\partial \phi}{\partial x}, \quad w = \frac{\partial \phi}{\partial z}. \quad (23)$$

Incompressibility requires that the velocity potential ϕ satisfy the Laplace equation (1).

In the dynamic boundary condition, we now include

the nonlinear terms in the hydrodynamic pressure acting on the ice and in the deflection of the ice cover, so that it reads

$$B\frac{\partial^2}{\partial x^2}\left(\frac{1}{R}\right)+\frac{Q}{R}+M\frac{\partial^2\eta}{\partial t^2} = -\frac{\partial\phi}{\partial t}-g\eta-\frac{u^2+w^2}{2}, \quad \text{at} \quad z=\eta \tag{24}$$

where R is the radius of curvature and is given by

$$\frac{1}{R}=\frac{\partial^2\eta}{\partial x^2}\Big/\left[1+\left(\frac{\partial\eta}{\partial x}\right)^2\right]^{3/2}. \tag{25}$$

The quantities B, Q and M have been defined earlier. Let us now change to a coordinate system moving with the phase speed of the waves. We imagine a basic current with velocity potential $\phi=-Cx$ in the x-direction and a superimposed steady finite wave motion. Then the time derivative on the right side of Eq. (24) reappears as spatial derivative, and the second time derivative on the left side can be written as a space derivative and incorporated into the compression term. By assuming that the surface slope is small and only including terms up to third order, the dynamic boundary condition becomes

$$\left[B\frac{\partial^4}{\partial x^4}+Q_0\frac{\partial^2}{\partial x^2}+g\right]\eta = -\frac{u^2+w^2}{2}+\frac{3}{2}B\left[\frac{\partial^4\eta}{\partial x^4}\left(\frac{\partial\eta}{\partial x}\right)^2+6\frac{\partial\eta}{\partial x}\frac{\partial^2\eta}{\partial x^2}\frac{\partial^3\eta}{\partial x^3}+2\left(\frac{\partial\eta}{\partial x^2}\right)^3\right]+\frac{3}{2}Q\frac{\partial^2\eta}{\partial x^2}\left(\frac{\partial\eta}{\partial x}\right)^2, \quad \text{at} \quad z=\eta \tag{26}$$

where $Q_0=Q+MC^2$, and we have used

$$\left[1+\left(\frac{\partial\eta}{\partial x}\right)^2\right]^{-3/2}=1-\frac{3}{2}\left(\frac{\partial\eta}{\partial x}\right)^2. \tag{27}$$

The kinematic boundary condition also needs to be satisfied at the bottom of the ice, rather than at $z=0$, and the condition for a steady wave motion is

$$w=\frac{d\eta}{dt}=(-C+u)\frac{\partial\eta}{\partial x} \quad \text{at} \quad z=\eta. \tag{28}$$

We now express ϕ, η and the phase speed as power series of the small (amplitude) parameter ϵ:

$$\phi=-Cx+\epsilon\phi^{(1)}+\epsilon^2\phi^{(2)}+\epsilon^3\phi^{(3)}+\cdots \tag{29a}$$

$$\eta=\epsilon\eta^{(1)}+\epsilon^2\eta^{(2)}+\epsilon^3\eta^{(3)}+\cdots \tag{29b}$$

$$C=C_0+\epsilon C_1+\epsilon^2C_2+\cdots. \tag{29c}$$

We shall expand Eqs. (27) and (28) in Taylor series around $z=0$; for a term ( ) that is

$$(\ )_{z=\eta}=(\ )_{z=0}+\eta\left[\frac{\partial}{\partial z}(\ )\right]_{z=0}+\frac{\eta^2}{2}\left[\frac{\partial^2}{\partial z^2}(\ )\right]+\cdots. \tag{30}$$

Carrying out the expansions and equating terms of the same power in ϵ, we obtain a sequence of equations for successively higher order terms.

The first-order approximation yields the equations

$$\nabla^2\phi^{(1)}=0, \tag{31a}$$

$$\left[g+B\frac{\partial^4}{\partial x^4}+Q_0\frac{\partial^2}{\partial x^2}\right]\eta^{(1)}-C_0\phi_x{}^{(1)}=0 \quad \text{at} \quad z=0, \tag{31b}$$

$$-C_0\eta_x{}^{(1)}-\phi_z{}^{(1)}=0 \quad \text{at} \quad z=0. \tag{31c}$$

The first-order solutions are

$$\eta^{(1)}=a\sin kx, \tag{32a}$$

$$\phi^{(1)}=-aC_0e^{kz}\cos kx, \tag{32b}$$

where

$$C_0{}^2=g_0/k; \quad g_0=g+Bk^4-Q_0k^2$$

$$\sigma_0{}^2=g_0k. \tag{33}$$

These are the same first-order results as obtained before, however they are now the result of a formal expansion process, and the higher order dynamics can also be analyzed.

For the second-order terms, we have the following three equations

$$\nabla^2\phi^{(2)}=0, \tag{34a}$$

$$\left[g+B\frac{\partial^4}{\partial x^4}+Q_0\frac{\partial^2}{\partial x^2}\right]\eta^{(2)}-C_1\phi_x{}^{(1)}-C_0\phi_x{}^{(2)}+\frac{1}{2}\phi_x{}^{(1)2}+\frac{1}{2}\phi_z{}^{(1)2}-C_0\eta^{(1)}\phi_{xz}^{(1)}=0 \quad \text{at} \quad z=0 \tag{34}$$

$$-C_0\eta_x{}^{(2)}-C_1\eta_x{}^{(1)}+\phi_x{}^{(1)}\eta_x{}^{(1)}-\phi_z{}^{(2)}-\eta^{(1)}\phi_{zz}^{(1)}=0 \quad \text{at} \quad z=0. \tag{34c}$$

The solutions at the second order are as follows:

$$\phi^{(2)}=\phi_2e^{kz}\sin 2kx, \tag{35a}$$

$$\eta^{(2)}=\eta_2\cos 2kx. \tag{35b}$$

Next, we solve for the unknown constants ϕ_2 and η_2. First, we combine Eqs. (34b) and (34c) to give

$$\left[g+B\frac{\partial^4}{\partial x^4}+Q_0\frac{\partial^2}{\partial x^2}\right]\phi_z{}^{(2)}+C_0{}^2\phi_{xx}^{(2)}+2C_1akg_0\cos kx-a^2kC_0(15Bk^4-3Q_0k^2)\sin 2kx=0. \tag{36}$$

One may conclude that

$$C_1=0, \tag{37a}$$

$$\phi_2=\frac{a^2kC_0(15Bk^4-3Q_0k^2)}{g+15Bk^4-3Q_0k^2}, \tag{37b}$$

$$\eta_2 = \frac{a^2 g_0 k(-g + 45Bk^4 - 9Q_0k^2)}{2(g + 15Bk^4 - 3Q_0k^2)(g + 16Bk^4 - 4Q_0k^2)}. \quad (37c)$$

It is to be noted that for open-ocean conditions, $B = Q' = 0$, we have $\phi_2 = 0$ and $\eta_2 = -a^2k/2$. The presence of a second-order potential function is thus peculiar to waves on an ice-covered sea. The third-order terms give the equations:

$$\nabla^2\phi^{(3)} = 0, \quad (38a)$$

$$\left[g + B\frac{\partial^4}{\partial x^4} + Q_0\frac{\partial^2}{\partial x^2}\right]\eta^{(3)} - \frac{3}{2}B\left[\eta_{xxxx}^{(1)}\eta_x^{(1)2} + 6\eta_x^{(1)}\eta_{xx}^{(1)}\eta_{xxx}^{(1)} + 2\eta_{xx}^{(1)3}\right] - \frac{3}{2}\eta_x^{(1)2}\eta_{xx}^{(1)} - C_0\phi_x^{(3)}$$
$$- C_1\phi_x^{(2)} - C_2\phi_x^{(1)} + \phi_z^{(1)}\phi_z^{(2)} - C_1\eta^{(1)}\phi_{xz}^{(1)} + \eta^{(1)}\phi_x^{(1)}\phi_{xz}^{(1)} + \eta^{(1)}\phi_z^{(1)}\phi_{zz}^{(1)}$$
$$- C_0\eta^{(2)}\phi_{xz}^{(1)} - \frac{1}{2}C_0\eta^{(1)2}\phi_{xzz}^{(1)} + \phi_x^{(1)}\phi_x^{(2)} = 0, \quad (38b)$$

$$-C_2\eta_x^{(1)} + \eta_x^{(1)}\phi_x^{(2)} - C_1\eta_x^{(2)} + \eta_x^{(2)}\phi_x^{(1)} - C_0\eta_x^{(3)} - \phi_z^{(3)}$$
$$+ \eta^{(1)}\eta_x^{(1)}\phi_{xz}^{(1)} - \phi_{zz}^{(2)}\eta^{(1)} - \eta^{(2)}\phi_{zz}^{(1)} - \frac{1}{2}\eta^{(1)2}\phi_{zzz}^{(1)} = 0. \quad (38c)$$

Taking the x-derivative of Eq. (38b) and operating on Eq. (38c) with the operator $(g + B\partial^4/\partial x^4 + Q_0\partial^2/\partial x^2)$, and then equating the coefficient of $\cos kx$ to zero, we obtain, after some algebraic manipulation

$$2g_0C_2 = a^2k^2C_0[g + 127Bk^4 - 10Q_0k^2 - 3Qk^2]$$
$$- 36k\eta_2C_0[10Bk^4 - Q_0k^2]$$
$$- 2k\phi_2[7g + 187Bk^4 - 25Q_0k^2]. \quad (39)$$

These results enable us to calculate the coefficients in the nonlinear cubic Schrödinger equation (22).

We have for γ, which expresses effect of the dependence of wave speed upon amplitude, the value (Mei 1983)

$$\gamma = C_2k/a^2. \quad (40)$$

If γ is positive, the wave speed increases with amplitude, while if γ is negative the wave speed decreases with increasing amplitude.

The other constant β provides the dispersive effect discussed by Mei (1983)

$$\beta = -\frac{1}{2}\frac{\partial^2\sigma}{\partial k^2}$$
$$= \{g^2(1 + 4kM) - 6gBk^4(5 + 8kM + 4k^2M^2)$$
$$+ 2gQk^2(3 + 2kM + 2k^2M^2) - 3Q^2k^4$$
$$- B^2k^8(15 - 20kM + 8k^2M^2)\}/$$
$$[8\sigma^3(1 + kM)^4]. \quad (41)$$

This should be compared to the open water surface values which are, for $B = Q_0 = 0$,

$$\gamma = \frac{1}{2}\sigma_0k^2, \quad (42a)$$

and

$$\beta = \frac{1}{8}\sigma_0/k^2. \quad (42b)$$

It is worth noting that the signs of both these crucial coefficients can change with ice parameters, and that it is possible to change the character of the higher order wave dynamics (Liu and Benney 1981).

The main results of the preceding analysis of weakly nonlinear waves are

1) The presence of a second harmonic dependence in the velocity potential showing that waves on ice-covered water differ from Stokes waves, although the waves still are waves of permanent type in the sense that they preserve their shape in the same manner as Stokes waves.

2) The new terms in the equation for modulational dynamics, the nonlinear cubic Schrödinger equation, showing that ice parameters enter into the wave modulation process. As shown in the next sections, the growth rate of wave packets on an initially uniform amplitude wave train on ice-covered water can be many times higher than that for open water.

8. The Weddell Sea example

We again return to the Weddell Sea case to compare the analytical results with observations. For the Weddell sea case, we have a value of $\gamma = -2.15 \times 10^{-3}$ m^2 s^{-1}, which compares to an open water value with the same wave period, $\gamma = 3 \times 10^{-5}$ m^2 s^{-1}. This shows that there is a change in sign and an increase of two orders of magnitude from open water to the Weddell sea ice conditions.

Figure 2 shows the effects of compression and flexural stiffness on the nonlinear wave speed. Notice that when $\lambda > 285$ m, the wave speed increases with increasing amplitude due to the nonlinear wave speed term C_2 being positive. Now for the case $\lambda < 285$ m, the wave speed decreases with amplitude since the second order correction C_2 is negative. Figure 3 shows the

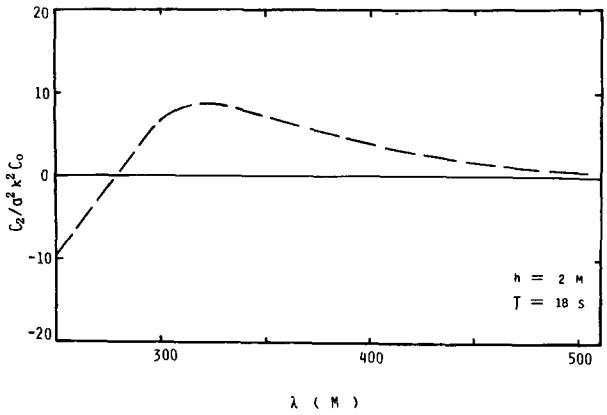

FIG. 2. Ice compressive and flexural effects on nonlinear wave speed with ice thickness $h = 2$ m and wave period $T = 18$ sec.

nonlinear and dispersive coefficients for wave modulation. $\beta\lambda > 0$ for almost all wavelengths except near the wavelength of 290 m. As demonstrated next in the stability analysis, a uniform wave train is unstable if $\beta\gamma > 0$, and a finite amplitude wave packet will emerge. Therefore, waves of 18 sec period are unstable for almost all values of compressive stress; the stress determines the wavelength plotted in the figure.

9. Stability analysis

The stability analysis of Benjamin and Feir (1967) can be carried out using the nonlinear cubic Schrödinger equation, which in a frame moving at group velocity can be written

$$\frac{\partial S}{\partial t} + i\beta \frac{\partial^2 S}{\partial x^2} + i\gamma S^2 S^* = 0. \tag{22}$$

Take a uniform wave train of constant amplitude as the initial condition,

$$S_0 = a \exp(-ia^2\gamma t). \tag{43}$$

Now introduce small sideband perturbations, letting the field be described as

$$S = \{a + be^{i(\Delta kx - \Omega t)} + de^{-i(\Delta kx - \Omega t)}\} \exp\{-i\gamma a^2 t\}, \tag{44}$$

where $a \gg b$, $a \gg d$, and $k \gg \Delta k$. Substituting Eqs. (44) into (22) and linearizing about the state S_0 results in the relation

$$\Omega^2 = (\Delta k)^2(\beta^2 \Delta k^2 - 2\beta\gamma a^2). \tag{45}$$

The question of stability now reduces to determining the sign of Ω^2. Clearly, Ω^2 is positive whenever $\beta\gamma < 0$, and then the wave train is stable to sideband perturbations. When $\beta\gamma > 0$, the stability boundary is at values of Δk given by

$$\Delta k = \sqrt{2}a(\gamma/\beta)^{1/2}. \tag{46}$$

The instability domain is then given by

$$0 < \Delta k/k < \sqrt{2}a/k(\gamma/\beta)^{1/2}. \tag{47}$$

The maximum instability occurs for

$$\Delta k = \Delta k_{\max} = a(\gamma/\beta)^{1/2}, \tag{48}$$

with the maximum growth rate given by

$$(\mathrm{Im}\Omega)_{\max} = |\gamma| a^2. \tag{49}$$

For the Weddell Sea case, we find that $(\mathrm{Im}\Omega)_{\max} = 2.1 \times 10^{-3}\ \mathrm{s}^{-1} = 1/(8\ \mathrm{min})$ for waves of one meter amplitude and $\Delta k_{\max} = 0.0023\ \mathrm{m}^{-1} = 2\pi/(3\ \mathrm{km})$. These results indicate that the e-folding time of modulational instability is 8 minutes and the wave packet length is about 3 km. The formation of wave packets takes place much faster than in open water. It should be noted that the experimental results of Lake and Yuen (1977) for modulational development in open-water wave fields agreed with the predictions obtained from the Schrödinger equation. The larger growth rate that we find for the Weddell Sea case suggests that wave packet formation in a region of high compressive stress may be a contributory element in ice breakup and pressure ridge formation.

10. Refraction of waves at the ice edge

Wind waves are generated in the open ocean, and the waves that penetrate into the ice pack have received their energy from the wind before they encounter the ice pack. The open-ocean wind wave field results from a complicated combination of linear and nonlinear processes. The wave field is broadband both in frequency and wavenumber, and propagates over a range of directions. For low values of compressive stress, Eq. (6) shows that the wave propagation speed is higher inside the ice pack than that in the open water. This makes total reflection possible for certain wavenumbers and directions of impingement. Based on Snell's law, waves that propagate in a direction with an angle to the normal larger than θ_c, where the critical angle satisfies

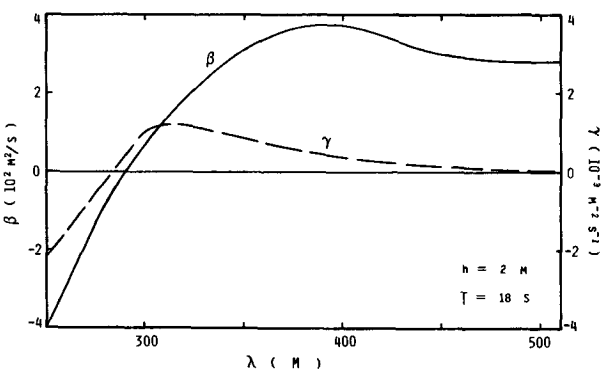

FIG. 3. Nonlinear and dispersive effects on wave modulation with ice thickness $h = 2$ m and wave period $T = 18$ sec.

$$\sin\theta_c(\sigma) = k_2(\sigma)/k_1(\sigma), \tag{50}$$

will be totally reflected. The subscript 1 stands for the value of the wavenumber in the open ocean, while the subscript 2 denotes the value inside the ice pack.

In order to further illustrate how the critical angle for total reflection varies with wave frequency, one takes its derivative with respect to frequency, to obtain

$$\cos\theta_c \frac{d\theta_c}{d\sigma} = \frac{1}{k_1}\left(\frac{1}{C_{g2}} - \frac{2}{C_2}\right). \tag{51}$$

When there is no compressive stress in the ice pack, such as in the marginal ice zone, the wave group velocity is always higher than one half of the phase speed as evident from Eq. (11). Therefore, according to Eq. (51) $d\theta_c/d\sigma$ is always negative, which means that the shorter (high frequency) waves will tend to be totally reflected at incidence angles closer to the normal than would be the case for waves of lower frequency. Refraction of waves from the ice edge is thus selective in wavelength; longer waves being transmitted while shorter waves are totally reflected for a given incidence angle.

When a wave is totally reflected, its momentum component normal to the ice pack edge also has to be reversed. This requires a stress upon the wave field, and its reaction will be found as a sum of mean current momentum and compressive stress in the ice pack.

11. Discussion

As reported by E. Augstein, the chief scientist of the *Polarstern* in the Weddell Sea, the effects of the wave arrival were impressive; in a few hours the previously continuous ice cover was split into small floes, with few floes being over 50 m in diameter. P. Wadhams and V. Squire also made some wave measurements after the pack stress had been relieved by failure in the ice pack and wave-induced breakup. They found wavelengths in the range of 500 to 600 meters while the wave period stayed more or less the same. It is interesting to note that this dispersion relation fits the open-water wave case. This would apply once the ice cover had broken up and no longer would be able to support compressive stress.

The observation reported from the *Polarstern* while in the Weddell Sea has provided a touchstone for our analysis of wave dispersion with the effects of compression and ice thickness added. We have shown that wave energy can be concentrated because of pack compression through two very different mechanisms, namely a very small group velocity caused by high compressive stress and the increased instability of nonlinear modulations also caused by pack compression. The very high growth rate involved in wave packet formation under high compressive stress is surprising, and it may be significant in the process of ice cover breakup and pressure ridge formation.

The other effect discovered in modulational dynamics, namely the sign reversals of both the last two terms in the nonlinear cubic Schrödinger equation, is difficult to interpret physically. One then wonders if a wave packet initially steepens at the forward or backward side, and, when a wave packet involves initial ice failure, if the packet radically changes its structure and causes intensive rafting. There are a number of such unanswered questions left. An important remaining problem is the rate of wave damping. As shown in the Appendix, the viscous damping for a uniform amplitude train of waves is not necessarily modest, so waves should not be able to penetrate 560 km into the ice pack without possible focusing effects as demonstrated in the nonlinear development of wave packets.

We may therefore speculate about the sequence of processes that cause ice pack breakup, pressure ridge formation and the formation of open bands of water. First, pack compression seems an important parameter. Pack compression can result from the radiation stress from waves totally reflected at the pack edge and from strong wind stress by storm. Compressive stress can also be caused by wave damping, since waves will have to give up their momentum to the mean stress and velocity fields. Then, due to two-dimensional inhomogeneities in the ice field, waves may be focused as from a lens, and because of pack compression, waves can be concentrated by caustic formation, where the group speed approaches zero. The wave energy concentration due to the convergence in the wave energy density, aided by the stronger tendency to form wave packets can lead to pack failure and wave dissipation. The momentum carried by these waves and the strong wind stress from storm can then push individual ice floes together and form rafts and pressure ridges. A reduction in flexural stiffness due to rafting, i.e., floes sliding over one another, may also be accompanied by a reduction of the compressive stress.

The next wave train coming in may encounter pressure ridges, while the leads may have closed due to residual pack stresses. The pressure ridge, while being a region of thicker ice, is insufficiently consolidated to have a large flexural stiffness, since the rafted floes may still slide over one another, and will have relatively low group velocity. Wave energy may concentrate and further contribute to pack failure, rafting and ridge growth may occur. Figure 4 illustrates the interactions between waves, pack modification through momentum transfer, the effects of pack parameters on wave processes, and the resulting rafting and pressure ridge formation from wind and waves. This description is highly idealized and oversimplified, but the results of our analysis suggest that all the needed elements for such a process are present. Also, our analysis suggests an explanation for the change in wave dispersion observed from the ship between the time of first arrival of the waves and after the pack was partially broken up by the first waves. The example offered by the Weddell Sea observations

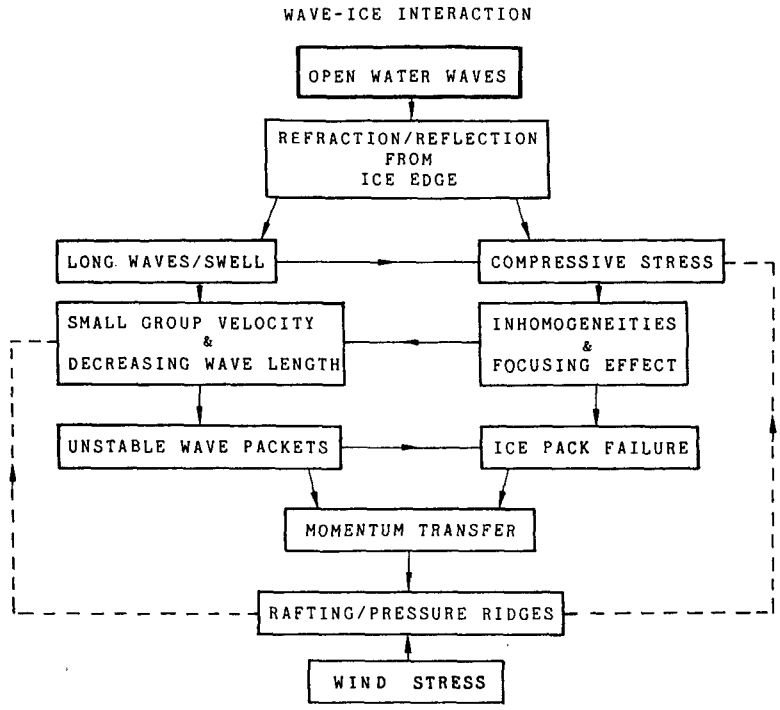

FIG. 4. Schematic diagram of wave-ice interaction.

lends some more realism to the analysis, and we suggest that our results may prove useful in designing experiments to investigate ice pack dynamics, and may also serve as a guide to attempts at parameterization of ice pack processes.

Acknowledgments. We thank Dr. E. Augstein of the Alfred Wegener Institute fur Polar und Meeresforschung for bringing the Weddell Sea wave event observed from the *Polarstern* to our attention and for sending us the observational data. We also thank Dr. F. Ostapoff, Dr. S. Ackley, and Dr. J. Comiso for useful discussions and exchanges of views. We would like to also acknowledge Dr. P. Wadhams and Dr. V. Squire for providing additional observational data. The reviewers' suggestions and comments are very much appreciated.

APPENDIX A

Viscous Attenuation of Swell by an Ice Sheet

The direct calculation of the effects of viscosity on wave propagation using a streamfunction and a velocity potential can be carried out as follows. Introduce the potential

$$\phi = Ae^{kz} \exp[i(kx + nt)], \tag{A1}$$

and streamfunction

$$\Psi = De^{mz} \exp[i(kx + nt)], \tag{A2}$$

here, n is a complex angular frequency. Using the linearized form of the Navier-Stokes equation written in terms of the streamfunction:

$$\frac{\partial \Psi}{\partial t} = \nu \nabla^2 \Psi, \tag{A3}$$

This gives

$$m^2 = k^2 + n/\nu, \tag{A4}$$

where ν is the kinematic viscosity of water.

The kinematic boundary conditions (28) results in

$$\eta = \frac{k}{n}(A + iD) \exp(ikx + nt). \tag{A5}$$

The linearized dynamic boundary condition when the effects of viscosity are included, is

$$\left[B\frac{\partial^4}{\partial x^4} + Q\frac{\partial^2}{\partial x^2} + M\frac{\partial^2}{\partial t^2}\right]\eta = -\frac{\partial \phi}{\partial t} - g\eta - 2\nu\frac{\partial w}{\partial z}, \tag{A6}$$

where

$$u = \frac{\partial \phi}{\partial x} - \frac{\partial \Psi}{\partial z}, \quad w = \frac{\partial \phi}{\partial z} + \frac{\partial \Psi}{\partial x}. \tag{A6}$$

Consider the ice to be a thin elastic plate with negligible extension in the outer fibers. The inclusion of viscosity requires no-slip at the ice-water interface, i.e.,

$$ikA - mD = 0. \tag{A7}$$

By substituting (A1), (A2), (A5) and (A7) into (A6), we obtain

$$-(Bk^4 - Qk^2 + Mn^2 + g)k(1 - k/m) = n^2. \quad \text{(A8)}$$

Eliminate m using Eq. (A4) to find

$$[n^2(1 + kM) + kP]^2 + n\nu k^2[n^2(1 + 2kM) + 2kG] = 0, \quad \text{(A9)}$$

where $G = g + Bk^4 - Qk^2$.

If $k^2\nu \ll \sigma$, to a first order approximation, we recover the dispersion relation $n_0 = \pm i\sigma$, where σ is given by Eq. (6).

For the second-order approximation, we have

$$n_1 = -\frac{\sqrt{\nu}k\sqrt{\sigma}}{2\sqrt{2}(1 + kM)}, \quad \text{(A10)}$$

where the correction to the dispersion (imaginary part) is neglected. It is to be noted that, for a free surface case $B = M = Q = 0$, this attenuation rate reduces to

$$n_1 = -\frac{\sqrt{\nu}k\sqrt{\sigma}}{2\sqrt{2}}. \quad \text{(A11)}$$

This agrees with the result of Phillips (1977) who analyzed the case of waves under a layer of densely packed surface film of very viscous oil.

This temporal decay rate can be converted to a spatial decay rate through the group velocity C_g, as originally done by Gaster (1962), and it gives

$$\alpha_x = n_1/C_g. \quad \text{(A12)}$$

For wave damping in the presence of very thin brash-ice layer, i.e., $\sigma^2 = gk$, Eq. (A12) reduces to the result by Weber (1987).

In the Weddell Sea, if using $\nu = 1.8 \times 10^{-6}$ m^2 s^{-1} for the kinematic viscosity of water, we have

$$n_1 = 0.67 \times 10^{-5}\ \text{s}^{-1} = 1/(41.5\ \text{h}). \quad \text{(A13)}$$

For an average C_g of 4 m s^{-1}, we find

$$\alpha_x = 1/(600\ \text{km}). \quad \text{(A14)}$$

However, the ice–water interface is rough with rafting and ridging activities. In general, the boundary layer beneath the ice is turbulent and in which the small-scale processes may be parameterized by an eddy viscosity coefficient. The eddy viscosity is not a physical but a phenomenological parameter, which can only be determined as a function of the flow conditions. In the Arctic Ocean, the eddy viscosity was estimated by Brennecke (1921) to be 160 cm^2 s^{-1} under the ice, and by Hunkins (1966) to be 24 cm^2 s^{-1} from ice drift.

For a 250 m wave with average C_g of 4 m s^{-1} in the ice pack and $\nu_e = 24$ cm^2 s^{-1}, the decay rate is

$$\alpha_x = 1/(17\ \text{km}). \quad \text{(A15)}$$

In the marginal ice zone with negligible compression stress, the decay rate is

$$\alpha_x \approx 1/(120\ \text{km}) \rightarrow 1/(50\ \text{km}) \quad \text{(A16)}$$

for a 510 m wave with $C_g \approx 15$ m s^{-1} and $\nu_e \approx 24 \rightarrow 160$ cm^2 s^{-1}. These results of damping rate compare reasonably well with observations in the marginal ice zone (Wadhams 1978; Weber 1987) for shorter waves. These results show that waves can not penetrate far into the pack without possible focussing effects as discussed in the nonlinear development of wave packets. However, the damping rate (A16) may be overestimated for a continuously covered ice sheet due to the use of large eddy viscosity.

REFERENCES

Benjamin, T. B., and J. E. Feir, 1967: The disintegration of wave trains on deep water. *J. Fluid Mech.*, **27**, 417–430.

Brennecke, B., 1921: Die Ozeanographischen Arbeiten der Deutschen Antarktischen Expedition 1911–1912. *Arch. Dtsch. Seewarte*, **39**, 206.

Forbes, L. K., 1986: Surface waves of large amplitude beneath an elastic sheet. Part 1: High-order series solution. *J. Fluid Mech.*, **169**, 409–428.

Gaster, M., 1962: A note on the relation between temporally-increasing and spatially-increasing disturbances in hydrodynamic instability. *J. Fluid Mech.*, **14**, 222–224.

Hunkins, K., 1986: Ekman drift current in the Arctic Ocean. *Deep-Sea Res.*, **13**, 607–620.

Lake, B. M., and H. C. Yuan, 1977: A note on some nonlinear water wave experiments and comparison of data with theory. *J. Fluid Mech.*, **83**, 75–81.

Liu, A. K., and S. H. Davis, 1977: Viscous attenuation of mean drift in water waves. *J. Fluid Mech.*, **81**, 63–84.

Liu, A. K., and D. J. Benney, 1981: The evolution of nonlinear wave trains in stratified shear flows. *Stud. Appl. Math.*, **64**, 247–269.

Mei, C. C., 1983: *The Applied Dynamics of Ocean Surface Waves.* Wiley & Sons, 740 pp.

Mellor, M., 1983: Mechanical behavior of sea ice. *Cold Reg. Res. Eng. Lab. Monogr.*, 83-1, 105 pp.

Mollo-Christensen, E., 1983a: Edge waves as a cause of ice ride-up on shore. *J. Geophys. Res.*, **88**, 2967–2970.

——, 1983b: Interaction between waves and mean drift in an ice pack. *J. Geophys. Res.*, **88**, 2971–2972.

Phillips, O. M., 1977: *The Dynamics of the Upper Ocean.* 2nd ed., Cambridge University Press, 336 pp.

Squire, V. A., 1984: A theoretical, laboratory, and field study of ice-coupled waves. *J. Geophys. Res.*, **89**, 8069–8079.

Tse, F. S., I. E. Morse and R. T. Hinkle, 1978: *Mechanical Vibrations Theory and Applications,* 2nd ed., Allyn & Bacon, 269 pp.

Wadhams, P., 1973: Attenuation of swell by sea ice. *J. Geophys. Res.*, **78**, 3552–3563.

——, 1978: Wave decay in the marginal ice zone measured from a submarine. *Deep-Sea Res.*, **25**, 23–40.

——, V. A. Squire, J. A. Ewing and R. W. Pascal, 1986: The effect of the marginal ice zone on the directional wave spectrum of the ocean. *J. Phys. Oceanogr.*, **16**, 358–376.

Weber, J. E., 1987: Wave attenuation and wave drift in the marginal ice zone. *J. Phys. Oceanogr.*, **17**, 2351–2361.

Whitham, G. B., 1974: *Linear and Nonlinear Waves.* Wiley and Sons, 636 pp.

Yuen, H. C., and B. M. Lake, 1975: Nonlinear deep water waves: Theory and experiment. *Phys. Fluids*, **18**, 956–960.

Zakharov, V. E., and A. B. Shabat, 1972: Exact theory of two-dimensional self-focusing and one-dimensional self-modulation of waves in nonlinear media. *Sov. Phys. JETP*, **34**, 62–69.